

IEEE TRANSACTIONS ON ELECTROMAGNETIC COMPATIBILITY

A PUBLICATION OF THE IEEE ELECTROMAGNETIC COMPATIBILITY SOCIETY



AUGUST 2009

VOLUME 51

NUMBER 3

IEMCAE

(ISSN 0018-9375)

PART I OF TWO PARTS

SPECIAL ISSUE ON LIGHTNING

GUEST EDITORIAL

Guest Editorial Special Issue on Lightning V. A. Rakov and F. Rachidi 426

SPECIAL ISSUE PAPERS

Overview

Overview of Recent Progress in Lightning Research and Lightning Protection (*Invited Paper*) V. A. Rakov and F. Rachidi 428

Lightning Discharge—Observations

Some Parameters of Negative Upward-Initiated Lightning to the Gaisberg Tower (2000–2007) (*Invited Paper*) G. Diendorfer, H. Pichler, and M. Mair 443

On the Current Peak Estimates Provided by Lightning Detection Networks for Lightning Return Strokes to Tall Towers (*Invited Paper*) D. Pavanello, F. Rachidi, W. Janischewskyj, M. Rubinstein, V. O. Shostak, C. A. Nucci, K. L. Cummins, A. M. Hussein, and J.-S. Chang 453

Lightning Electric Field Characteristics Associated With Transmission-Line Faults in Winter (*Invited Paper*) ... M. Ishii and M. Saito 459

Electromagnetic Pulses Produced by Bouncing-Wave-Type Lightning Discharges (*Invited Paper*) A. Nag and V. A. Rakov 466

Lightning Discharge—Modeling

New Insights Into Lightning Return-Stroke Models With Specified Longitudinal Current Distribution (*Invited Paper*) G. Maslowski and V. A. Rakov 471

Electric and Magnetic Fields Predicted by Different Electromagnetic Models of the Lightning Return Stroke Versus Measured Fields (*Invited Paper*) Y. Baba and V. A. Rakov 479

Representation of a Lightning Return-Stroke Channel as a Nonlinearly Loaded Thin-Wire Antenna (*Invited Paper*) S. H. Seyed Moosavi, R. Moini, and S. H. Hesam Sadeghi 488

(Contents Continued on Page 425)



Celebrating 125 Years
of Engineering the Future

IEEE ELECTROMAGNETIC COMPATIBILITY SOCIETY

The Electromagnetic Compatibility Society is an organization, within the framework of the IEEE, of members with principal professional interest in electromagnetic compatibility. All members of the IEEE are eligible for membership in the Society and will receive this TRANSACTIONS, upon payment of the annual Society membership fee of \$30.00. For information on joining, write to the IEEE at the address below. *Member copies of Transactions/Journals are for personal use only.*

BOARD OF DIRECTORS

Executive Officers

E. JOFFE, *President*
J. LASALLE, *Treasurer*

J. N. O'NEIL, *Secretary* (425) 868-2558
A. DROZD, *Past President*

Vice Presidents

T. HUBING, *Communications Services*
R. DAVIS, *Member Services*
J. NORGARD, *Standards* (719) 495-0359

R. SCULLY, *Technical Services*
G. PETTIT, *Conferences*

Directors-at-Large

2009

T. HUBING
D. SWEENEY
D. STAGGS

T. YOSHINO
R. SCULLY
R. GOLDBLUM

2010

M. MONTROSE
F. HEATHER
C. BRENCH

F. MARADEI
R. DAVIS
R. JOST

IEEE TRANSACTIONS® ON ELECTROMAGNETIC COMPATIBILITY

Editor-in-Chief

PERRY F. WILSON
NIST, Boulder, CO

Advisory Board

MARCELLO D'AMORE
University of Rome "La Sapienza"
Italy

PIERRE DEGAUQUE
Lille Univ. Sci. Tech.
France

SHUICHI NITTA
Tokyo Univ., Agriculture Technol.
Japan

CLAYTON R. PAUL
Mercer Univ.
Macon, GA, USA

FLAVIO G. CANAVERO
Polytechnic of Turin
Italy

Associate Editors

JOHAN CATRYSSÉ
KHBO-Oostende
Oostende, Belgium

C. CHRISTOPOULOS
Univ. Nottingham
Nottingham, U.K.

PAOLO CORONA
Naval Univ. Inst.
Napoli, Italy

X CUI
North China Electric Power Univ.
Baoding, China

J. DREWNIAK
Univ. Missouri-Rolla
Rolla, MO

A. DUFFY
De Montfort Univ.
Leicester, U.K.

OSAMU FUJIWARA
Nagoya Inst. Technol.
Nagoya, Japan

HEYNO GARBE
Univ. Hannover
Hannover, Germany

C. L. HOLLOWAY
NIST
Boulder, CO

JOUNGHO KIM
KAIST
Daejeon, Korea

NIELS KUSTER
Federal Inst. Technol.
Zurich, Switzerland

M. LEONE
Otto-von-Guericke Univ.
Magdeburg, Germany

ERPING LI
Univ. Singapore
Singapore

ANDY C. MARVIN
York Univ.
York, U.K.

S. PIGNARI
Polytechnic of Milan
Milan, Italy

FARHAD RACHIDI
Federal Inst. Technol.
Lausanne, Switzerland

VLADIMIR A. RAKOV
Univ. Florida
Gainesville, FL

M. S. SARTO
Univ. Rome "La Sapienza"
Rome, Italy

JAN LUIKEN TER HASEBORG
Technical Univ.
Hamburg-Harburg, Germany

O. WADA
Kyoto Univ.
Kyoto, Japan

IEEE Officers

JOHN R. VIG, *President*
PEDRO A. RAY, *President-Elect*
BARRY L. SHOOP, *Secretary*
PETER W. STAECKER, *Treasurer*
LEWIS M. TERMAN, *Past President*
TEOFILO RAMOS, *Vice President, Educational Activities*

JON G. ROKNE, *Vice President, Publication Services and Products*
JOSEPH V. LILLIE, *Vice President, Membership and Geographic Activities*
W. CHARLTON (CHUCK) ADAMS, *President, IEEE Standards Association*
HAROLD L. FLESCHER, *Vice President, Technical Activities*
GORDON W. DAY, *President, IEEE-USA*

ROGER W. SUDBURY, *Director, Division IV—Electromagnetics and Radiation*

IEEE Executive Staff

BETSY DAVIS, *SPHR, Human Resources*
ANTHONY DURNIAK, *Publications Activities*
JUDITH GORMAN, *Standards Activities*
CECELIA JANKOWSKI, *Member and Geographic Activities*
DOUGLAS GORHAM, *Educational Activities*

MATTHEW LOEB, *Corporate Strategy & Communications*
RICHARD D. SCHWARTZ, *Business Administration*
CHRIS BRANTLEY, *IEEE-USA*
MARY WARD-CALLAN, *Technical Activities*

IEEE Periodicals

Transactions/Journals Department

Staff Director: FRAN ZAPPULLA

Editorial Director: DAWN MELLEY *Production Director:* PETER M. TUOHY

Managing Editor: MARTIN J. MORAHAN *Senior Editor:* GEORGE CRISCIONE

IEEE TRANSACTIONS ON ELECTROMAGNETIC COMPATIBILITY (ISSN 0018-9375) is published quarterly by the Institute of Electrical and Electronics Engineers, Inc. Responsibility for the contents rests upon the authors and not upon the IEEE, the Society/Council, or its members. **IEEE Corporate Office:** 3 Park Avenue, 17th Floor, New York, NY 10016-5997. **IEEE Operations Center:** 445 Hoes Lane, Piscataway, NJ 08854-4141. **NJ Telephone:** +1 732 981 0060. **Price/Publication Information:** Individual copies: IEEE Members \$20.00 (first copy only), nonmembers \$100.00 per copy. (Note: Postage and handling charge not included.) Member and nonmember subscription prices available upon request. Available in microfiche and microfilm. **Copyright and Reprint Permissions:** Abstracting is permitted with credit to the source. Libraries are permitted to photocopy for private use of patrons, provided the per-copy fee indicated in the code at the bottom of the first page is paid through the Copyright Clearance Center, 222 Rosewood Drive, Danvers, MA 01923. For all other copying, reprint, or republication permission, write to Copyrights and Permissions Department, IEEE Publications Administration, 445 Hoes Lane, Piscataway, NJ 08854-4141. Copyright © 2009 by the Institute of Electrical and Electronics Engineers, Inc. All rights reserved. Periodicals Postage Paid at New York, NY and at additional mailing offices. **Postmaster:** Send address changes to IEEE TRANSACTIONS ON ELECTROMAGNETIC COMPATIBILITY, IEEE, 445 Hoes Lane, Piscataway, NJ 08854-4141. GST Registration No. 125634188. CPC Sales Agreement #40013087. Return undeliverable Canada addresses to: Pitney Bowes IMEX, P.O. Box 4332, Stanton Rd., Toronto, ON M5W 3J4, Canada. Printed in U.S.A.

Modeling of Grounding Electrodes Under Lightning Currents

Leonid Grcev, *Senior Member, IEEE*

(Invited Paper)

Abstract—More precise modeling of the dynamic performance of grounding electrodes under lightning currents must include both the time-dependent nonlinear soil ionization and the frequency-dependent phenomena. These phenomena might have mutually opposing effects since the soil ionization effectively improves, while frequency-dependent inductive behavior impairs, the grounding performance. Modern approaches that take into account both phenomena are based on circuit theory that does not allow for accurate analysis of high-frequency behavior. This paper aims to further improve the understanding of the dynamic behavior of grounding electrodes under lightning currents by focusing on the following aspects: analyzing the validity domains of popular modeling approaches, based on circuit, transmission line, and electromagnetic theory; providing parametric analysis that takes into account both the propagation and soil ionization effects; analyzing simple formulas for surge characteristics; and comparing the modeling with experimental data. A model and a simple formula that combine the electromagnetic approach, suitable for high-frequency analysis, with the method that accounts for the soil ionization effects, recommended by the International Council on Large Electric Systems (CIGRE) and the IEEE Working Groups, are used for the parametric analysis. Both the model and the simple formula are verified by comparison with experimental results available in the literature.

Index Terms—Frequency response, grounding, lightning, modeling, transient response.

I. INTRODUCTION

VERTICAL and horizontal grounding electrodes are traditionally used in lightning protection systems “to direct the lightning current from the down conductors to the earth with a minimum rise in the potential of the above-ground part of the protection system” [1]. The safety criteria based on “a minimum rise in the potential” are taken from power systems analysis [2]. However, in such a case, the usual dc approximation leads to rather straightforward computations. Fig. 1 shows a theoretical circuit for evaluation of the voltage that the above-ground part of the protective system attains in reference to remote earth. An ideal dc current source I is connected with one terminal to the grounding electrodes and with the other terminal to the remote earth, theoretically at infinite distance. The influence of the connecting leads is ignored. The voltage between the current source terminals is uniquely defined, and is equivalent to the electric potential of the ground electrodes V with a reference point at the remote earth. This enables definition of the low-frequency

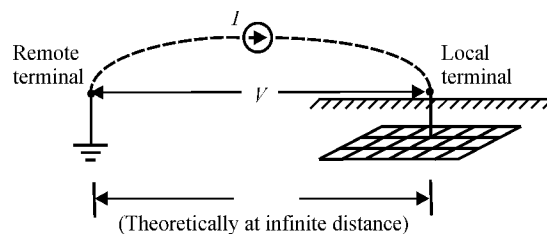


Fig. 1. Theoretical circuit for evaluation of a dc grounding resistance R .

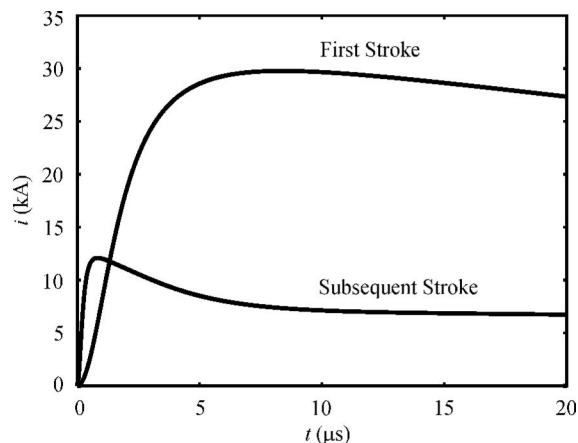


Fig. 2. Typical first and subsequent return stroke current waveforms [3].

grounding resistance R , which is given as

$$R = \frac{V}{I}. \quad (1)$$

Therefore, the goal of minimizing V is achieved by a design that minimizes R .

However, the situation is different in the case of lightning. Current that is injected in the grounding electrodes is a fast-varying current pulse with high peak values. For example, Fig. 2 shows two typical lightning current waveforms related to the first and subsequent strokes that will be used in this study [3]. The details of these lightning current waveforms are given in Section V-A.

The dynamic response of the grounding electrodes subjected to such current pulses is predominantly influenced by two physical processes, which are related to the following properties of the current pulse waveform:

- 1) the soil ionization in the immediate proximity of the grounding electrode, which is related to the current pulse intensity;

Manuscript received November 1, 2008. First published August 7, 2009; current version published August 21, 2009.

The author is with the Faculty of Electrical Engineering and Information Technologies, Ss. Cyril and Methodius University, Skopje 1000, Macedonia (e-mail: Leonid.Grcev@ieee.org).

Digital Object Identifier 10.1109/TEMC.2009.2025771

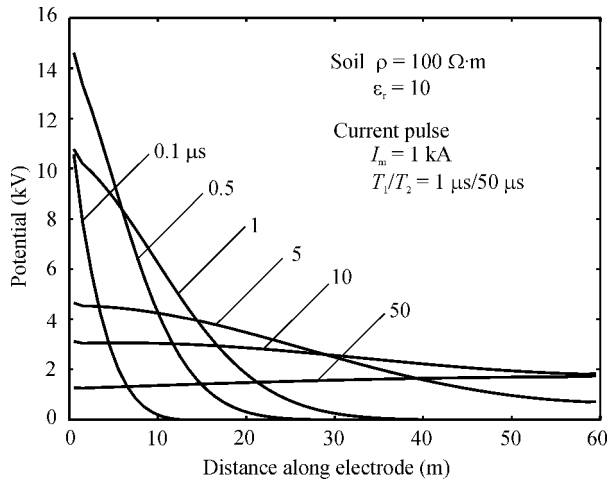


Fig. 3. Propagation of a potential pulse along 60 m horizontal grounding electrode when a current pulse is injected in wire's left end [5].

- 2) the lightning pulse propagation along the grounding electrode, which is related to the current pulse front time.

In the case of a current pulse with a high peak value (e.g., such as the first stroke current pulse in Fig. 2), the electric field at the ground electrodes may become larger than the electric strength of the soil, resulting in breakdown and spark discharges. This results in “lowering the grounding resistance by effectively enlarging the size of the electrode” [1], and therefore, in improving the grounding performance in comparison to the low-current cases.

On the other hand, when fast front current pulses (e.g., such as the subsequent stroke current pulse in Fig. 2) are injected in the electrode, due to the limited speed of current pulse propagation along the electrode, only a small part of the electrode is effective in discharging the current to the earth in the first moments of the pulse. This might result in large values of leakage currents and potentials near the current injection point, and the grounding performance might be impaired in comparison to the low-frequency cases [4].

This effect is illustrated in Fig. 3 (with soil ionization effects ignored) [5]. The figure shows the propagation of conductor potentials along the electrode as a response to a current pulse injected in one end of the horizontal 60-m-long electrode. Snapshots of computer animation are shown at six moments of time after the beginning of the current injection (at $t = 0.1, 0.5, 1, 5, 10,$ and $50 \mu\text{s}$).

Two periods might be distinguished: 1) surge period—before the pulse reaches the other end of the electrode, when only part of the electrode is effective in discharging the current to earth, characterized by large values and uneven distributions of the potential and 2) stationary period—after the pulse reaches the other end of the electrode, characterized by even distributions, when the whole electrode is effective in discharging the current to earth. The latter period in most cases is very similar to the low-frequency case.

Attempts at more precise modeling of the dynamic performance of grounding electrodes under lightning currents must include both soil ionization and propagation phenomena. Nev-

ertheless, existing methods often separately analyze either the effects of soil ionization, e.g., [6]–[9], or the effects of pulse propagation, e.g., [10]–[14]. On the other hand, the existing modeling approaches that include both phenomena are based either on circuit [15]–[17] or transmission-line theory [18]–[20], whose underlying assumptions limit their accuracy for fast front pulses that are crucial for the propagation effects. Although much work has been done by many researchers in the past 80 years on this subject “there is no consensus yet on how to apply this knowledge to the design of the actual electrode system” [21]. There is also no consensus even on the definition of the surge characteristics and the validity of the methods of analysis.

This paper aims to further improve the understanding of the dynamic behavior of grounding electrodes under lightning currents by focusing on the following aspects.

- 1) Clarifying the basic concepts underlying surge characteristics.
- 2) Analyzing the validity domains of popular modeling approaches.
- 3) Providing parametric analysis that simultaneously takes into account propagation and soil ionization effects.
- 4) Analyzing simple formulas for surge characteristics.
- 5) Validating the modeling with comparison to experiments.

We compare three popular models, based on circuit, transmission line, and electromagnetic theory, first in the frequency domain, and then, in the time domain for typical lightning current pulses. A parametric analysis is presented in the following ranges: earth's resistivity 10–10 000 $\Omega\cdot\text{m}$, electrode length 1–30 m, lightning current pulse zero-to-peak time 0.8 and 8 μs , and peak value 12 and 30 kA. To take into account both soil ionization and frequency-dependent effects, we use recently introduced procedure [42], [43] to combine compared models with an approximate soil ionization effects formula, as recommended by the International Council on Large Electric Systems (CIGRE) and IEEE Working Groups.

Finally, we analyze and discuss use of a new simple formula for surge characteristics that take into account both the phenomena. We also present comparison of the procedure and the formula with experimental data, and conclude that there exists a fairly good agreement.

For completeness, definitions of surge characteristics are summarized, and their significance is discussed in practical examples. Also, details of all analyzed methods are briefly described.

II. QUANTITIES USED TO CHARACTERIZE THE DYNAMIC PERFORMANCE OF GROUNDING ELECTRODES

It can be seen from Fig. 3 that complex spatial and temporal distributions are necessary for complete analysis of the dynamic behavior of grounding electrodes under lightning currents. In addition to potential distributions, longitudinal and leakage current, electromagnetic fields, and voltages are necessary in detailed electromagnetic compatibility (EMC) and safety studies, e.g., [22]–[25]. However, single quantities based on the time functions of the injected current $i(t)$ and the resulting electric potential at the injection point in relation to remote ground

$v(t)$ are mostly used. The main purpose of these quantities is to compare the dynamic performance with the low-frequency low-current performance [19].

The peak values of $i(t)$ and $v(t)$, I_m and V_m , respectively, are the basis for the definition of the quantity coined as impulse impedance Z , defined by

$$Z = \frac{V_m}{I_m} \quad (2)$$

where Z in (2) is related to the low-frequency grounding resistance R in (1) by the dimensionless impulse coefficient A given as

$$A = \frac{Z}{R}. \quad (3)$$

If the performance of the grounding electrode is equal in surge and low-frequency low-current conditions, then $Z = R$, and consequently, $A = 1$. Clearly, values of A larger than one indicate impaired surge performance, while values of A less than one indicate improved surge performance compared to the low-frequency grounding performance.

Since for longer grounding electrodes Z might become larger than R , i.e., A might become larger than one, the surge effective length ℓ_{eff} is defined as the maximal grounding electrode length for which A is equal to one [5], [26], [27].

Also, the quantity coined transient grounding impedance $z(t)$ is a time function defined as a quotient between $v(t)$ and $i(t)$ as

$$z(t) = \frac{v(t)}{i(t)}. \quad (4)$$

The practical meaning of these quantities will be discussed in Section V-C.

Another useful quantity is coined as the harmonic grounding impedance [52], [53]

$$Z(j\omega) = \frac{V(j\omega)}{I(j\omega)}. \quad (5)$$

This quantity is in the frequency domain, and $I(j\omega)$ and $V(j\omega)$ are phasors of the injected current and the potential at the injection point, respectively.

In contrast to the time-domain quantities in (2)–(4) that depend on the excitation waveform, $Z(j\omega)$ depends only on the geometric and electromagnetic properties of the electrodes and the medium. It is useful for the analysis of frequency-dependent effects with ionization ignored. As it is well known, $Z(j\omega)$ enables evaluation of the time functions of the potential $v(t)$ as a response to an arbitrary current pulse $i(t)$ by [22]

$$v(t) = \mathbb{F}^{-1} \{ \mathbb{F}[i(t)] Z(j\omega) \} \quad (6)$$

where \mathbb{F} and \mathbb{F}^{-1} denote Fourier and inverse Fourier transforms, respectively.

It is worth noting that quantities coined as “impedances,” Z in (2), $z(t)$ in (4), and $Z(j\omega)$ in (5), are not well-defined impedances in the electromagnetic textbooks since $v(t)$ and $V(j\omega)$ are not the voltages between the current source terminals in Fig. 1, but only potentials at the grounding electrode feed point. An important property of these quantities is that they reduce to the low-frequency grounding resistance R , e.g., $z(t)$ in

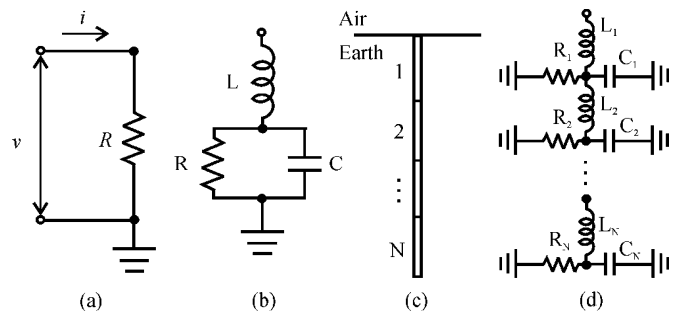


Fig. 4. Low-current models of a grounding electrode. (a) Low-frequency grounding resistance. (b) High-frequency lumped RLC circuit. (c) Segmented grounding electrode. (d) High-frequency segmented RLC circuit.

stationary period, and $Z(j\omega)$ for low-frequencies, and their deviation from R indicates differences between the dynamic and low-frequency grounding performance.

III. APPROACHES TO MODELING

In this section, three popular modeling approaches are briefly described based on circuit, transmission line, and electromagnetic theory. As most electrodes have a vertical or a horizontal position, we constrain the analysis to such cases. For simplicity, we consider only single electrodes. In the first part of this section, i.e., Section III-A, we consider the so-called low-current models that disregard effects of soil ionization, and in the next part, i.e., Section III-B, we consider the models that take into account soil ionization.

A. Frequency-Dependent Effects

1) *Circuit Approach:* In the low-frequency case, static analysis is usually applied, which leads to the well-known formulas for the grounding resistance R [see Fig. 4(a)]. Therefore, for the vertical electrode, according to Dwight [29]

$$R \text{ (in ohms)} = \frac{\rho}{2\pi\ell} \left[\ln \left(\frac{4\ell}{a} \right) - 1 \right] \quad (7a)$$

and for the horizontal electrode, according to Sunde [30]:

$$R \text{ (in ohms)} = \frac{\rho}{\pi\ell} \left[\ln \left(\frac{2\ell}{\sqrt{2ad}} \right) - 1 \right] \quad (7b)$$

where ρ is resistivity of the earth (in ohms-meter), ℓ is grounding electrode length (in meters), a is radius (in meters), and d is depth of burial of horizontal electrodes (in meters), assuming $\ell \gg a$ and $\ell \gg d$. R in (7) is derived by applying the static image method.

A simple lumped-circuit high-frequency model suggested by Rudenberg [4] is illustrated in Fig. 4(b). R is computed by (7) and the grounding capacitance C is computed based on the relationship [30]

$$C \text{ (in farads)} = \frac{\rho\epsilon}{R} \quad (8)$$

where ϵ is permittivity of the soil (in farads per meter).

As mentioned in [30, p. 257], the inductance L of a horizontal wire reduces slightly as the depth of the wire is increased.

Therefore, for horizontal “wires at ordinary depths, the inducances are substantially the same as for wires at the surface” [30, p. 114] given as

$$L \text{ (in henries)} = \frac{\mu\ell}{2\pi} \left[\ln \left(\frac{2\ell}{a} \right) - 1 \right] \quad (9)$$

where μ is permeability of the soil (in henries per meter), which is usually assumed to be equal to the permeability of a vacuum. The same formula is used also for vertical electrodes [31]. Use of alternative approximation formulas for L is discussed in [28].

The additional underlying assumptions in the aforementioned formulas are a uniform charge distribution along the electrodes in (7) and (8), and a uniform longitudinal current distribution in (9) [30].

The electrode is often divided into N fictitious segments to take into account the nonuniform distributions of the charge and current, and each segment of the electrode is represented by an RLC section [32], as illustrated in Fig. 4(c) and (d).

2) *Transmission-Line Approach*: The most popular transmission-line approach model is an extension of the circuit model [see (7)–(9)]. Per-unit-length parameters are approximately determined, according to [30], as

$$\begin{aligned} R' \text{ (in ohms meter)} &= \frac{1}{G'} = R\ell \\ C' \text{ (in farads per meter)} &= \frac{C}{\ell} \\ L' \text{ (in henries per meter)} &= \frac{L}{\ell} \end{aligned} \quad (10)$$

where R , C , and L are determined by (7), (8), and (9), respectively.

Both circuit and transmission-line models can be used for computations in the time and frequency domains. In the frequency domain, the transmission line may be considered as open, and the harmonic grounding impedance is [33]

$$Z(j\omega) = Z_0 \coth \gamma\ell \quad (11a)$$

$$Z_0 = \sqrt{\frac{j\omega L'}{G' + j\omega C'}} \quad \gamma = \sqrt{j\omega L'(G' + j\omega C')} \quad (11b)$$

where $j = \sqrt{-1}$, $\omega = 2\pi f$, and f is the frequency (in hertz). In (11) and Section III-A3, the time variation $\exp(j\omega t)$ is suppressed.

Since both circuit and transmission-line models are based on quasi-static approximation, their validity is limited at high frequencies.

3) *Electromagnetic Approach*: The most popular electromagnetic approach is based on antenna theory and the method of moments (MOMs) [22]. This method is based on an exact solution of the electromagnetic fields of a Hertzian dipole in or near a lossy half-space [34], and therefore, is based on fewer neglected quantities in comparison to the previous models. This is a full-wave frequency-domain approach; however, its basic requirement is that the system is linear. Therefore, this method is not suited for the modeling of nonlinear phenomena. On the other side, it is well suited for modeling frequency-dependent characteristics [22].

The details of the MOM are available elsewhere [35]. Here, the method will only be briefly described. It is assumed that electrodes are thin, and that current and charge densities along electrodes are approximated by filaments of current and charge on the electrode axis. Each electrode is thought of as divided in segments, as illustrated in Fig. 4(c). An impedance matrix $[Z]$ is then obtained using the MOM to describe the electromagnetic interactions between segments. $[Z]$ is an $N \times N$ matrix, where N is the number of segments. In this process, the electromagnetic field equations are reduced to a matrix form [25] as

$$[Z][I] = I_s [Z'] \quad (12)$$

where $[I]$ is a column matrix whose elements are unknown phasors that approximate the current distribution along electrodes, I_s is the phasor of the injected current, and $[Z']$ is a column matrix whose elements are impedances between the segment, where the current is injected, and all the other segments [25].

The grounding harmonic impedance $Z(j\omega)$ is

$$Z(j\omega) = \frac{V_s}{I_s} = \frac{[I]^T [Z'] + I_s Z_s}{I_s} \quad (13)$$

where V_s is the phasor of the potential at the injection segment in reference to remote ground and Z_s is the self-impedance of the injection segment.

The key step is the evaluation of the elements of the $[Z]$ matrix in (12), which can be written in the following general form [36]:

$$z_{mn} = \int_m \int_n F_m F_n G_{mn} dl_m dl_n \quad (14)$$

where F_m and F_n are the functions related to the approximation of the current and the boundary conditions along the m th and n th segments, respectively. G_{mn} is the Green's function, which is equivalent to the electromagnetic field at the n th segment due to a current element in the m th segment. For evaluation of G_{mn} , the exact Sommerfeld's solution [34] is used. G_{mn} can be cast in the following form [37]:

$$G_{mn} = g_{mn} + K g'_{mn} + S_{mn} \quad (15)$$

where g_{mn} is the Green's function for the current element below the ground in an unbounded homogeneous lossy medium with earth's characteristics and g'_{mn} for its image above the earth's surface. Applying only g_{mn} and g'_{mn} in (15) would be equal to the method of static images. K in (15) is coefficient that modifies the images [25] and S_{mn} involves Sommerfeld-type integrals [34]. The latter term converges to zero for low frequencies, but becomes significant at high frequencies. The first term of (15), g_{mn} , can be expressed as [35]

$$g_{mn} = \frac{\exp(-jkr)}{r}, \quad k = \omega \sqrt{\left(\epsilon - \frac{j}{\omega\rho} \right) \mu} \quad (16)$$

where r is the distance between the source (at the m th segment) and the observation point (at the n th segment). One approximation of g_{mn} in (16) can be obtained by expanding the exponential

in a Maclaurin series [35] as

$$g_{mn} = \frac{1}{r} - jk - \frac{k^2}{2}r + \dots \quad (17)$$

The first term is identical to the static case. Therefore, if we would like to reduce the electromagnetic to the circuit approach, we could only use the first term in (17), static image theory in (15), and unit pulse functions for F_m and F_n in (14).

Solution of (12) gives the current and charge distribution along electrodes at a given frequency, which can be used for further computations of quantities of interest, such as potentials, voltages, fields, impedances, etc. In the frequency domain, these quantities may be considered as the system functions, and time responses can be obtained by (6) [22].

B. Nonlinear Soil Ionization Effects

1) *Nonlinear Grounding Resistance*: Bellaschi *et al.* [6] have determined the nonlinear relationship between the grounding electrode injected current and resistance, and proposed that it is a result of soil ionization at high-current values. They have concluded that soil ionization effectively increases the dimensions of the electrode; thus, decreasing the resistance. Based on the further work of Korsuntcev [38], and Eriksson and Weck [54], the following formula for a nonlinear resistance $R(t)$ (in ohms) as a function of the injected current i (in kiloamperes) is recommended in [40], [41], and [56]:

$$R(t) = \frac{R}{\sqrt{1 + i(t)/I_g}} \quad I_g = \frac{E_0 \rho}{2\pi R^2} \quad (18)$$

where E_0 is the earth's critical electric field intensity (in kilovolts per meter), ρ is the resistivity of the earth (in ohms-meter), and R is the low-frequency low-current grounding resistivity (in ohms) [see (1)]. Different values are recommended for E_0 , e.g., 300 kV/m in [40] and 400 kV/m in [41], although "values from 300 to 1500 kV/m have been used by various investigators" [56]. It should be emphasized that (18) has been recommended for electrodes with lengths of up to about 30 m [40].

The nonlinear resistance [see (18)] has also been used in the sequenced *RLC* model [see Fig. 4(d)], where linear R has been replaced by nonlinear $R(t)$ to include both high-frequency and soil ionization effects [32].

2) *Approximate Procedure for Simultaneous Time- and Frequency-Dependent Analysis*: Recently, a simplified procedure that takes into account both the time-dependent nonlinear effects of soil ionization and the frequency-dependent effects has been proposed [42], [43]. This procedure comprises two steps. The first step is to compute the potential at the injection point $v(t)$ as a response to an injected current $i(t)$, with ionization effects ignored, by any frequency-domain method, such as described in Section III-A. In this paper, $i(t)$ has a waveform illustrated in Fig. 2 and characteristics described in Section V-B. Then, two components of $v(t)$ are considered

$$v(t) = Ri(t) + x(t) \quad (19)$$

where R is the low-frequency grounding resistance [see (1)]. If the grounding electrode performs in surge conditions exactly as it performs at low frequencies, then (19) becomes: $v(t) =$

$Ri(t)$. Therefore, $x(t)$ in (19) reflects the difference between the surge and low-frequency performance. Consequently, the first component on the right side of (19) might be considered as an approximation of the resistive voltage drop in the ground, while the second component $x(t)$ is related to the frequency-dependent phenomena, and is mostly an approximation of the combination of the inductive and capacitive voltage drop in the earth.

The second step is to determine the total potential $v_i(t)$ that accounts for the soil ionization as

$$v_i(t) = R(t)i(t) + x(t) \quad (20)$$

i.e., by replacing R in (19) with nonlinear $R(t)$ in (20). Here, $R(t)$ is computed by (18) and $x(t)$ is derived from (19). Assuming that the ionization has the largest effect on the resistive voltage drop in the ground, these effects are ignored in $x(t)$. This simplified approach is validated by comparison to experiments in Section VII and [43]. However, its application is limited to the ranges of parameters given in Table II.

IV. COMPARISON BETWEEN MODELS IN THE FREQUENCY DOMAIN

In this section previously described models are compared in the frequency domain. Concerning the circuit model, it was demonstrated recently in [44] that the lumped circuit model, illustrated in Fig. 4(b), largely overestimates the harmonic impedance at high frequencies, and this model is not considered here anymore. In this paper, the following three models are compared.

- 1) A segmented *RLC* model, illustrated in Fig. 4(c) and (d), where the total number of segments N depends on the total electrode length where all segments are with equal length of 1 m [see (7)–(9)], denoted "*RLC*" in Figs. 5–11 (the length of the segment of 1 m is chosen just as an example—smaller or larger lengths would lead to better or worse agreement with the transmission-line model, respectively).
- 2) A transmission line model [see (10)–(11)] denoted "*TL*" in Figs. 5–11.
- 3) An electromagnetic model [see (12)–(16)] denoted "*EMF*" in Figs. 5–11.

The computation results by the three models for vertical grounding electrodes are presented in Figs. 5–7 for different lengths of the electrode and different resistivities of the earth. Fig. 5 shows the computation results for an electrode length of 1 m, Fig. 6 shows the computation results for an electrode length of 10 m, and Fig. 7 shows the computation results for an electrode length of 30 m. In all the cases, the electrode is constructed of copper with a diameter of 2.5 cm. In Figs. 5–7, results for four values of the earth's resistivity are presented: 10, 100, 1000, and 10 000 Ω -m. In all the cases, the relative permittivity of the earth is 10.

The presented results in Figs. 5–7 are normalized modulus of the harmonic impedance to the value of the low-frequency resistance in a frequency range from 100 Hz to 10 MHz. Presented frequency characteristics exhibit well-known behavior.

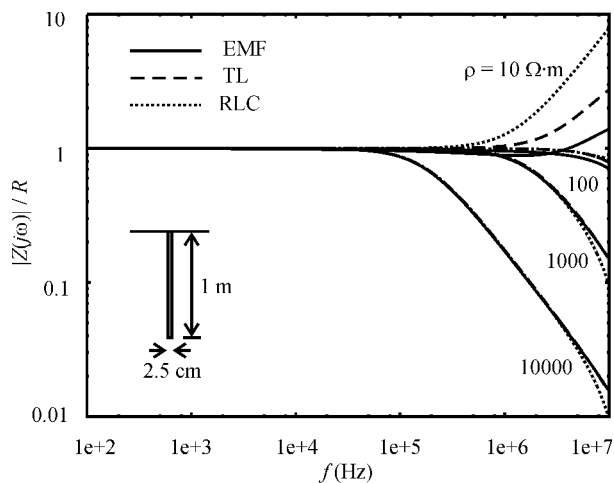


Fig. 5. Normalized modulus of the harmonic impedance to low-frequency resistance for a vertical electrode with length 1 m.

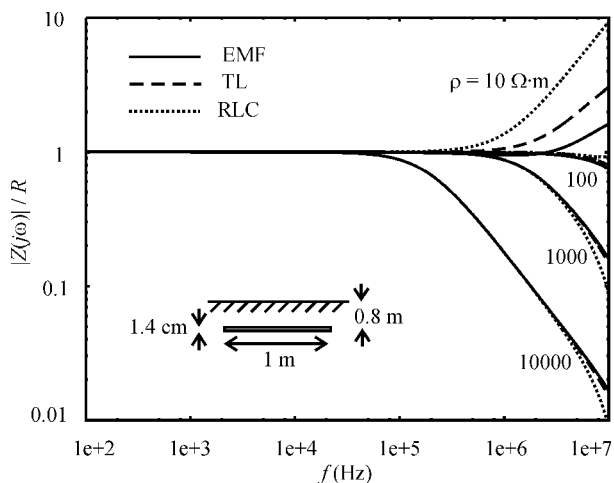


Fig. 8. Normalized modulus of the harmonic impedance to low-frequency resistance for a horizontal electrode with length 1 m.

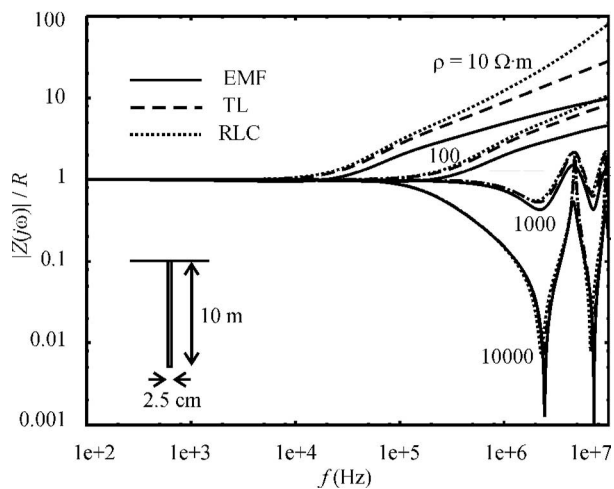


Fig. 6. Normalized modulus of the harmonic impedance to low-frequency resistance for a vertical electrode with length 10 m.

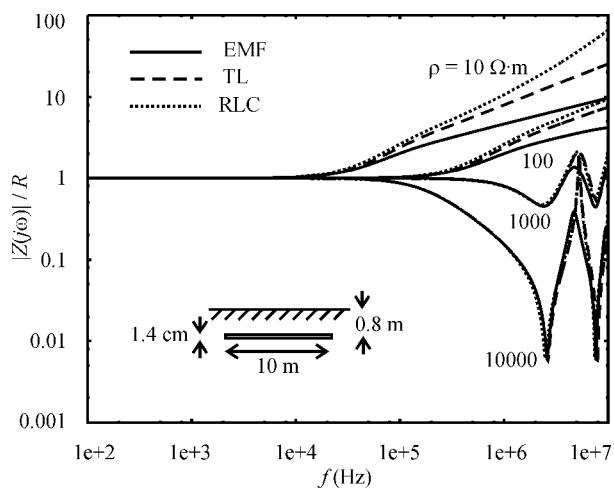


Fig. 9. Normalized modulus of the harmonic impedance to low-frequency resistance for a horizontal electrode with length 10 m.

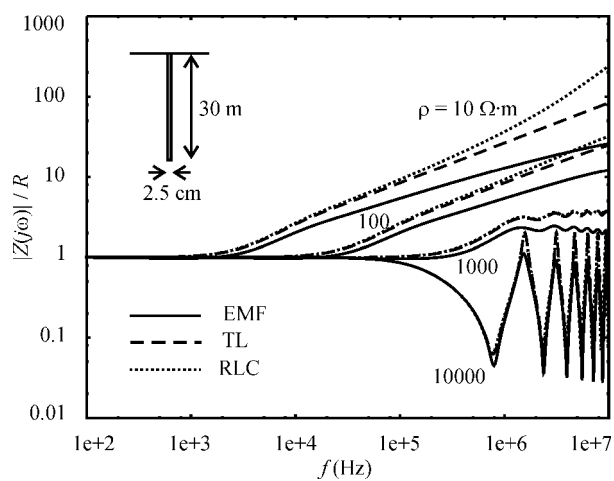


Fig. 7. Normalized modulus of the harmonic impedance to low-frequency resistance for a vertical electrode with length 30 m.

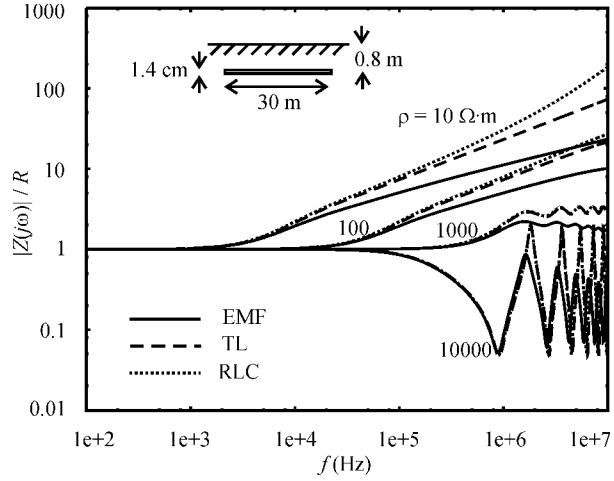


Fig. 10. Normalized modulus of the harmonic impedance to low-frequency resistance for a horizontal electrode with length 30 m.

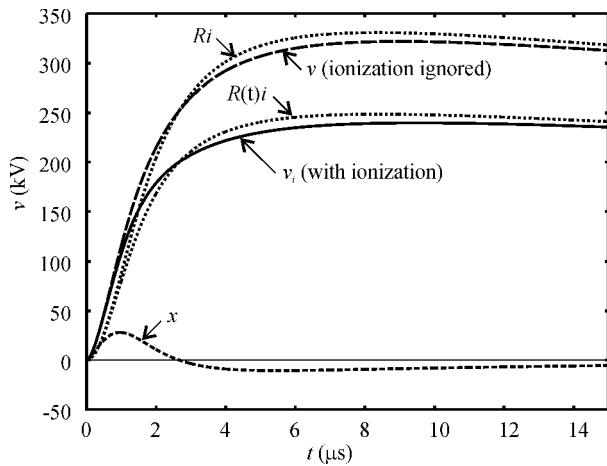


Fig. 11. Computed components of the potential at the injection point for first stroke current injected in a 10-m-long electrode in earth with $\rho = 100 \Omega\cdot\text{m}$.

- 1) At low frequencies, the grounding performance is frequency-independent ($Z(j\omega) \approx R$) up to some switch frequency.
- 2) Above the switch frequency, the grounding performance is frequency-dependent, either dominantly inductive ($|Z(j\omega)| > R$) or dominantly capacitive ($|Z(j\omega)| < R$).

As it is well known, high-frequency inductive behavior indicates a possibility that grounding performance might worsen in the first few moments of the lightning pulse; however, only if the lightning current waveform has enough frequency content above the switch frequency. On the contrary, the high-frequency capacitive behavior indicates a possibility of better grounding performance in the first few moments of the lightning pulse.

Figs. 8–10 are similarly organized, but for horizontal grounding electrodes. Here, the diameter is 1.4 cm and depth of burial is 0.8 m. Comparing results of Figs. 5–7 with Figs. 8–10 for the electrodes with the same length, it is obvious that, in spite of the differences in R , their high-frequency behavior is very similar.

All electrodes exhibit inductive behavior in more conducting earth and switch to capacitive behavior in more resistive earth. Of primary interest is inductive behavior, since it can impair the grounding performance. The switch frequency between the resistive and the inductive behavior was denoted as a characteristic frequency F_c by Gary [45]. However, Gary determined F_c by using circuit model and an alternative formula to (9) for L for horizontal electrodes, thus obtaining somewhat larger values. An empirical formula for F_c is derived in [46] using the electromagnetic model

$$F_c = \rho (0.6/\ell)^{2.3} \quad (21)$$

where F_c is in megahertz, ρ is in ohms-meter, and ℓ is in meters.

Comparing the results from the three models, they are similar for vertical electrodes that exhibit capacitive behavior. The differences are more significant for the inductive behavior when circuit and transmission-line models overestimate the inductive behavior in comparison to the electromagnetic model. The segmented circuit and transmission-line models mutually agree

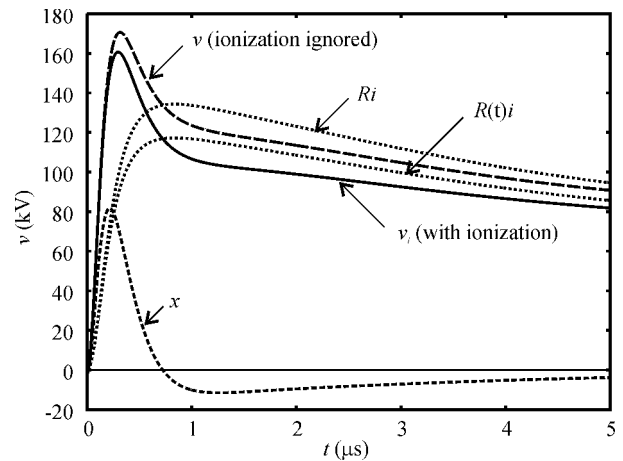


Fig. 12. Computed components of the potential at the injection point for subsequent stroke current injected in a 10-m-long electrode in earth with $\rho = 100 \Omega\cdot\text{m}$.

well nearly in all cases, except in extremely conductive soil with resistivity $10 \Omega\cdot\text{m}$.

A practical question is: what is the significance of the differences between the three models in the time domain, i.e., when electrodes are subjected to lightning current pulses, taking into account both the effects of propagation and ionization. The answer to this question is one of the subjects of the next section.

V. COMPUTATIONS IN THE TIME DOMAIN

A. Characteristics of the Typical Lightning Current Waveforms Used in Computations

In this study, we have used two lightning current waveforms chosen by Rachidi *et al.* [3] to fit experimental data corresponding to the typical first and subsequent return strokes, based on observations of Berger *et al.* [47] (see Fig. 2). The first stroke current pulse is characterized by a peak value of 30 kA, zero-to-peak time of about $8 \mu\text{s}$, and a maximum steepness of $12 \text{ kA}/\mu\text{s}$, whereas the subsequent stroke current has a peak value of 12 kA, zero-to-peak time of about $0.8 \mu\text{s}$, and a maximum steepness of $40 \text{ kA}/\mu\text{s}$.

While the first stroke current has larger intensity, the subsequent stroke, which has larger rate of rise of the front, has higher frequency content. As a first approximation, Gary [45] has proposed that the first stroke current waveform's frequency content is below 100 kHz, and subsequent stroke's is above 1 MHz.

B. Simultaneous Computation of Frequency-Dependent and Soil Ionization Effects

Figs. 11 and 12 illustrate the computation procedure that takes into account both frequency-dependent and soil ionization effects described in Section III-B.2. The case is the same as in Fig. 9, a horizontal electrode with $\ell = 10 \text{ m}$, $a = 7 \text{ mm}$, $d = 0.8 \text{ m}$ in earth with $\rho = 100 \Omega\cdot\text{m}$, $\epsilon_r = 10$, and $E_0 = 300 \text{ kV}/\text{m}$. Note that the electromagnetic model is used in all examples illustrated in Figs. 11–14.

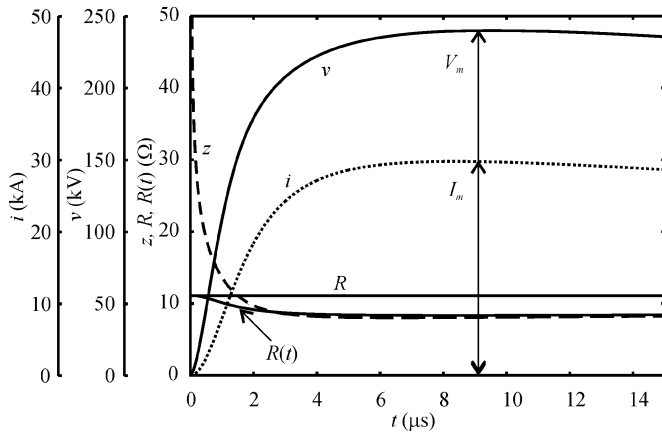


Fig. 13. Surge characteristics of a 10-m-long electrode in earth with $\rho = 100 \Omega\text{-m}$ for the first stroke current.

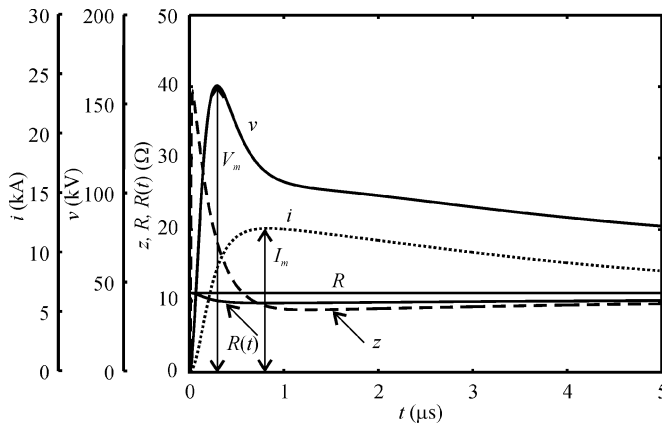


Fig. 14. Surge characteristics of a 10-m-long electrode in earth with $\rho = 100 \Omega\text{-m}$ for the subsequent stroke current.

The first step in the procedure is to compute the potential $v(t)$ [see (19)] with ionization ignored. It has two components: the pure resistive $Ri(t)$ and the reactive $x(t)$ part. Next, the total potential $v_i(t)$ [see (20)], with accounted soil ionization effects, is a sum of $R(t)i(t)$ and $x(t)$. The difference between $Ri(t)$ and $R(t)i(t)$ components represents the effects of soil ionization, and $x(t)$ represents the frequency-dependent effects.

The response of the same grounding electrode to the two different lightning current waveforms, related to the first (see Fig. 11) and subsequent (see Fig. 12) strokes, reveal important differences. The response to the first stroke (see Fig. 11) is dominantly resistive and soil ionization effects are dominant. This could also be concluded from an analysis of the harmonic impedance in Fig. 9. For resistivity of soil $100 \Omega\text{-m}$ and a frequency content of the first stroke current waveform below 100 kHz , the pulse is influenced only by the pure resistive behavior. Practically, the total potential $v_i(t)$ can be approximated with only the nonlinear resistive part $R(t)i(t)$.

However, the subsequent stroke, with frequency content above 1 MHz , is influenced by the inductive behavior, resulting in amplification of the high-frequency components and a large peak in the first moments of the potential pulse (see Fig. 12).

TABLE I
SURGE CHARACTERISTICS OF 10-m VERTICAL GROUNDING ELECTRODE IN EARTH WITH RESISTIVITY $100 \Omega\text{-m}$

	$R (\Omega)$	$Z (\Omega)$	A
First Stroke	11	8.3	0.75
Subsequent Str.	11	13.4	1.3

These effects are analyzed for a wider range of parameters and in more details in [43].

The effects of soil ionization start with the rise of the current, and the reduction of the total potential depends on the current peak intensity. This effect lasts during the large part of the pulse (see Fig. 11). However, in the case of the subsequent stroke (see Fig. 12), the inductive potential peak lasts only during the rise of the current pulse. In Fig. 12, this effect comes to its maximum before the soil ionization is fully developed, and consequently, soil ionization does not have a large effect in reducing the inductive potential peak.

C. Computation of Surge Characteristics

Figs. 13 and 14 illustrate the computation of the surge characteristics, for the same cases analyzed in Figs. 11 and 12, respectively.

The transient grounding impedance $z(t)$ [see (4)] in both cases in Figs. 13 and 14 rises fast to some large value in the initial surge period, after which it converges to the stationary condition characterized by values that may be approximated with $R(t)$ [see (18)]. This can be used to distinguish two periods of the transient response:

- 1) the initial surge period [when $z(t) \neq R(t)$];
- 2) the stationary period [when $z(t) \approx R(t)$].

Such division of the transient period is important, since the surge period is very short, from one to a few or few tens of microseconds, and the rest is the stationary period when the behavior may be approximated as dominantly resistive.

In the case of the first stroke (see Fig. 13), the potential pulse is not significantly modified in relation to the current pulse, and the dominantly resistive behavior results with the occurrence of the maximums of the current and the potential pulses in the same moment. In the case of the subsequent stroke inductive behavior results in the potential pulse leading the current pulse. The large peak of the potential pulse occurs only during the surge period. These differences are expressed by the different values of the surge characteristics (see Table I).

The meaning of the surge characteristics in relation to the dominant soil ionization or inductive effects is somewhat different (see Table I). In the case of the first stroke, the impulse coefficient $A < 1$ due to soil ionization, which reflects generally better grounding performance in relation to the low-frequency case. But in the case of the subsequent stroke, where $A > 1$ due to inductive effects, it reflects worsened performance in relation to the low-frequency case, but only during the surge period. In the rest of the pulse, the performance is slightly better than during the low-frequency case, but this is not reflected in the surge parameters.

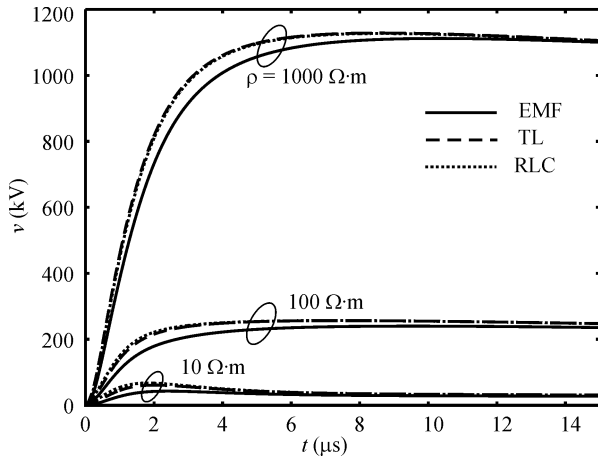


Fig. 15. First stroke current in a 10-m-long electrode.

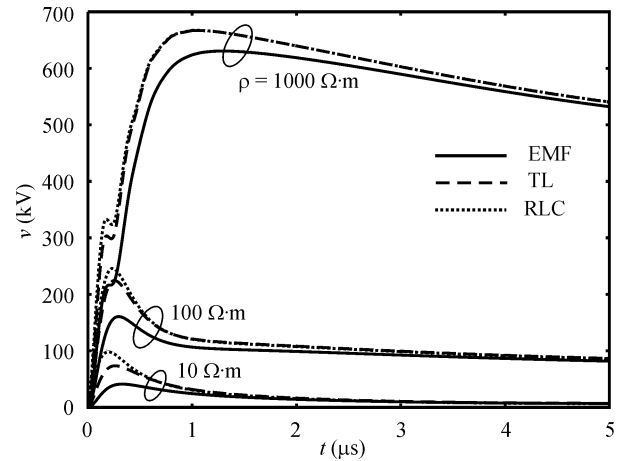


Fig. 17. Subsequent stroke current in a 10-m-long electrode.

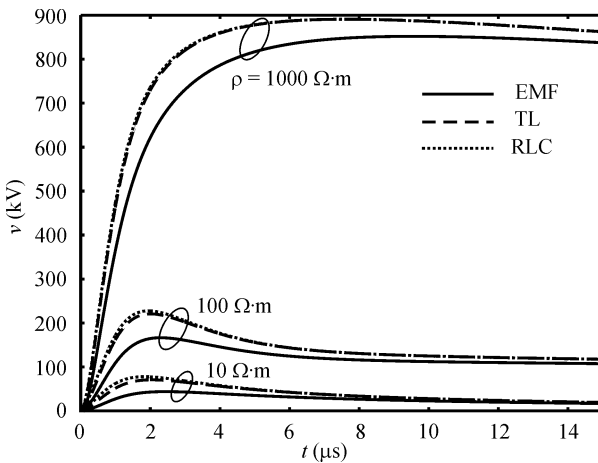


Fig. 16. First stroke current in a 30-m-long electrode.

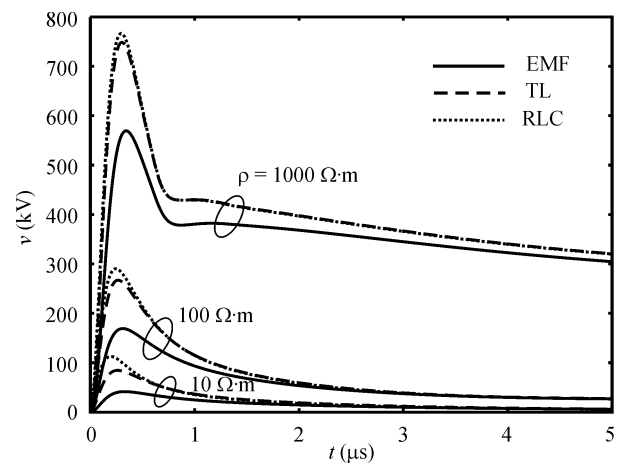


Fig. 18. Subsequent stroke current in a 30-m-long electrode.

D. Comparison Between Models in the Time Domain

Since the vertical and horizontal electrodes have very similar high-frequency behavior, only vertical electrode cases are used for comparison in the time domain. Note that computations in the time domain for the compared models were performed following the same procedure; first, $Z(j\omega)$ is computed by (11a) or (13), and then, $v(t)$ is determined by (6), and finally, (19) and (20) are applied.

Also, it is obvious that in the case of capacitive behavior, all models lead to similar results, and cases for electrode length $\ell = 1$ m and for other lengths in soil with $\rho = 10\,000 \Omega\cdot\text{m}$ are not used for further comparisons. The cases that are used for comparison of the three models are from Fig. 6 for electrode length $\ell = 10$ m and Fig. 7 for $\ell = 30$ m.

These electrodes are first subjected to the first stroke current pulse, and the results are shown in Fig. 15 (for electrode length $\ell = 10$ m) and Fig. 16 (for $\ell = 30$ m).

In all cases, circuit and transmission-line model overestimate the resulting potential in comparison to the electromagnetic model. Such overestimation is larger for inductive effects in the surge period; however, during the stationary period, the results from the different models mutually converge.

Next, the results when these electrodes are subjected to the subsequent stroke current pulse are shown in Fig. 17 (for electrode length $\ell = 10$ m) and Fig. 18 (for $\ell = 30$ m).

The conclusions here are similar to the cases of the first stroke current pulse, only the inductive effects occur in most of the analyzed cases. The differences are larger as the inductive effects are larger, but similarly, like in the first stroke case, after the surge period, the results by the different models mutually converge.

VI. SIMPLE FORMULA FOR THE IMPULSE COEFFICIENT

Recently, a new empirical formula for the impulse coefficient A [see (3)] has been proposed [42], [43]. First step is to compute the coefficients α and β [5], [26], [27]

$$\alpha = 0.025 + \exp(-0.82(\rho T_1)^{0.257}) \quad (22a)$$

$$\beta = 0.17 + \exp(-0.22(\rho T_1)^{0.555}) \quad (22b)$$

where, soil resistivity ρ is in ohms-meter and current pulse zero-to-peak time T_1 is in microseconds. Coefficients α and β do not have physical meaning; they are deduced from computer simulation results by the electromagnetic model.

TABLE II
INPUT PARAMETERS (25)

Parameter	Symbol	Unit	Validity range
Electrode length	ℓ	m	3 – 30
Soil resistivity	ρ	$\Omega \cdot \text{m}$	10 – 1000
Current pulse zero-to-peak time	T_1	μs	> 0.2
Current pulse peak value	I_m	kA	0 – 100
Soil critical E field	E_0	kV/m	300 – 1000

TABLE III
ELECTRODE AND SOIL PARAMETERS OF THE EXPERIMENTAL CASES

Case	Electrode	Soil
Fig. 19	Horizontal $\ell = 8 \text{ m}$ $a = 6 \text{ mm}$ $d = 0.6 \text{ m}$	$\rho = 65 \Omega \cdot \text{m}$ $\epsilon_r = 15$
Fig. 20	Horizontal $\ell = 5 \text{ m}$ $a = 4 \text{ mm}$ $d = 0.6 \text{ m}$	$\rho = 42 \Omega \cdot \text{m}$ $\epsilon_r = 10$ $E_0 = 350 \text{ kV/m}$
Fig. 21	Vertical $\ell = 2.5\text{--}10 \text{ m}$	$\rho = 20\text{--}2000 \Omega \cdot \text{m}$

Next, the effective length ℓ_{eff} (in meters) is determined by

$$\ell_{\text{eff}} = \left(\frac{1 - \beta}{\alpha} \right). \quad (23)$$

The impulse coefficient A with ionization ignored is

$$A = 1, \quad (\ell \leq \ell_{\text{eff}}) \quad (24a)$$

$$A = \alpha\ell + \beta, \quad (\ell \geq \ell_{\text{eff}}). \quad (24b)$$

Finally, the impulse coefficient A_i that takes into account both frequency-dependent inductive and time-dependent nonlinear behavior is determined by

$$A_i = \frac{1}{\sqrt{1 + I_m/I_g}} + A - 1, \quad I_g = \frac{E_0 \rho}{2\pi R^2} \quad (25)$$

where I_m is current pulse peak value in kiloamperes and A is computed by (24). Parameters on the right side of the relation for I_g are same as in (18). The validity domain of (25) is given in Table II.

The formula disregards effects that the soil ionization might have on the capacitive behavior; however, this may be considered as neglect on the “safe side” since capacitive behavior practically improves grounding performance by reducing $v_i(t)$ [20]. The simple formula in this section is applicable for vertical and horizontal electrodes. It can also be used for two- and four-arm horizontal arrangements and for single, two, and four driven rods arrangements using reduction factors given in [5, Table III].

The formula (25) can be compared with previously developed formulas for the impulse coefficient. One is the well-known

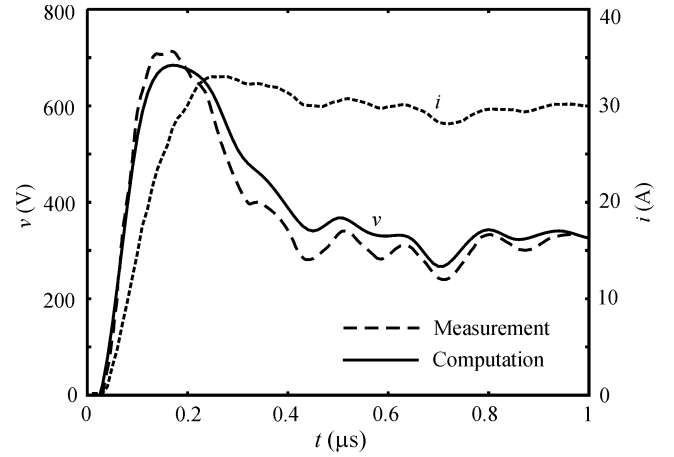


Fig. 19. Comparison with measurements by Electricité de France [50] (parameters are given in Table III).

formula by Gupta and Thapar [48]

$$A = \exp \left(0.333 \left(\frac{\ell}{\ell_{\text{eff}}} \right)^{2.3} \right), \quad \ell_{\text{eff}} = 1.4 \sqrt{\rho T_1}. \quad (26)$$

Another formula for the impulse coefficient of a linear horizontal conductor is developed in [49] as

$$A = 1.62 \rho^{-0.4} (0.5 + \sqrt{\ell}) [0.79 - \exp(-2.3 I_m^{-0.2})]. \quad (27)$$

However, (26) takes into account only frequency-dependent inductive effects and ignores soil ionization effects, and (27) ignores inductive effects, since it does not take into account T_1 that is crucial for the inductive effects. Formulas (26) and (27) also ignore the possibility of different values of E_0 .

Consequently, (25) is the most versatile amongst other previously derived formulas since it includes all the important parameters that characterize the dynamic behavior of grounding electrodes given in Table II.

VII. VALIDATION OF THE COMPUTATIONS

To validate the computations, they are compared with published experimental data as a reference. The values of the basic parameters of the experimental cases are given in Table III, and the comparisons between the simulation and experimental results are given in Figs. 19–21. Additional validation is also available elsewhere [43].

First, in Fig. 19, the electromagnetic model is compared with experimental results. Fig. 19 presents one of the rare carefully performed and well-documented experiments with fast front current with front time of about $0.2 \mu\text{s}$ that was carried out during the extensive field measurements performed in the mid-1980s by the Electricité de France [50], [52]. A low-intensity current pulse is injected in a grounding electrode i (dotted line), and the measured voltage to ground at the injection point v (broken line) clearly shows inductive effects. Computed v by the electromagnetic model (full line) agrees very well with the measurements. Additional validation of the electromagnetic model is also available elsewhere [25]. The measured and computed

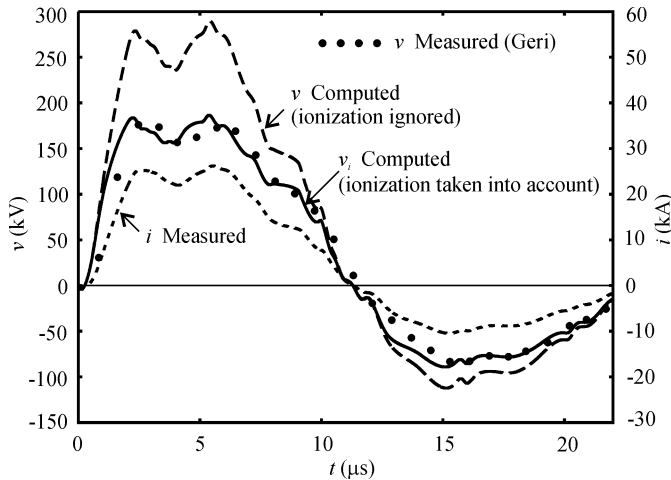


Fig. 20. Comparison with measured results for a horizontal electrode by Geri [15] (parameters are given in Table III).

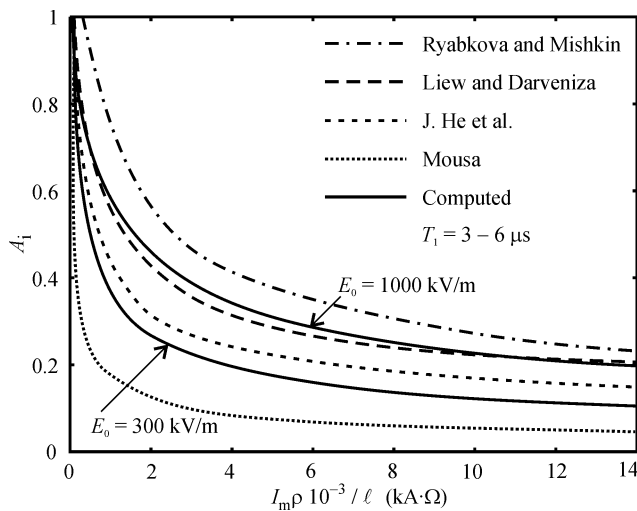


Fig. 21. Comparison with measurements by Ryabkova and Mishkin [51], Liew and Darveniza [8], He *et al.* [49], and Mousa [55], for $T_1 = 3 - 6 \mu\text{s}$ (parameters are given in Table III).

TABLE IV
COMPARISON OF MEASURED AND COMPUTED SURGE
CHARACTERISTICS IN FIG. 19

	R (Ω)	Z (Ω)	A
Measured	10	22	2.2
Computed – EM model	10	20.7	2.1
Computed – formula (25)			2.4

surge characteristics are given in Table IV. Formula (25) agrees reasonably well with measurements.

Next, Fig. 20 shows a comparison of the simulation and experimental results to validate the approximate procedure for simultaneous computation of soil ionization and frequency-dependent effects described in Section III-B.2. The reference case is from Geri's article [15, Fig. 14]. For the measured current pulse i injected into the electrode, the potential at the injection point v is computed when ionization is ignored by (19), and v_i when

the ionization is accounted for by (20). The simulated results for v_i are in good agreement with the experimental results.

Ryabkova and Mishkin [51] introduced a normalizing ratio $I_m \rho / \ell$ to present variation of the impulse coefficient A based on a comprehensive set of measurements for the case of a single vertical electrode, with current pulses with peak values in the range 10–100 kA and zero-to-peak time in the range of 3–6 μs (other parameters are given in Table III). Fig. 21 shows their generalized curve (it is a median line of scattered results). Liew and Darveniza in [8, Fig. 13], and Mousa in [55, Fig. 7] also predicted impulse characteristics of a single rod. For comparison reasons, their results have been normalized in a similar fashion in Fig 21. Also, in Fig. 21, the median line of the results by (27) of He *et al.* [49] for the same range of parameters is presented. Formula (27) is an empirical formula by regression analysis from a large amount of experimental results [49]. Therefore, these results present experimental results from four different research groups. There is a general agreement in the trend between presented experimental results; however, the four research groups have differently estimated the level of the grounding performance improvement due to the soil ionization. One explanation of such differences might be in the different approaches, e.g., Ryabkova and Mishkin results are from laboratory experiments on small-scale models.

To compare (25) with these experimental results, it is also presented with a median line of the results for two values of the critical electric field of the earth, 300 and 1000 kV/m.

VIII. DISCUSSION

The results in Fig. 21 show effects of only the soil ionization, since the values of the impulse coefficient are less than zero. It is a consequence of the rather slow front time in the range of 3–6 μs , which is too large for the induction effects to occur. The differences in experimental results by Ryabkova and Mishkin [51], Liew and Darveniza [8], Mousa [55], and He *et al.* [49] show that different approaches by different researchers predict more conservative or a more optimistic estimate of the effect of the soil ionization on the improvement of the grounding performance under high lightning current pulses. The results by (25) in Fig. 21 depend on the value of the parameter E_0 in (18). The parameter E_0 , the critical electric field of the earth, can be considered as a calibrating parameter in (25), which might be used to fit to more or less conservative experimental estimates of the soil ionization effect on the improvement of the grounding performance. It is worth noting that this possibility was mentioned by Oettle [39]. Recognizing that E_0 is difficult to estimate for different types of soils, it has been suggested that E_0 can be treated as an empirical calibrating factor [39, p. 2022]. Oettle selected $E_0 = 1000$ kV/m for her computations [39]; later, CIGRE Working Group [41] selected $E_0 = 400$ kV/m, while IEEE Working Group selected [40] $E_0 = 300$ kV/m. It might be an open question if a single value of E_0 should be used in all practical situations.

Unfortunately, there are no reliable experimental results in the literature that show simultaneously the soil ionization and inductive effects. For example, Fig. 19 shows only the inductive effects, while Figs. 20 and 21 show only the soil ionization

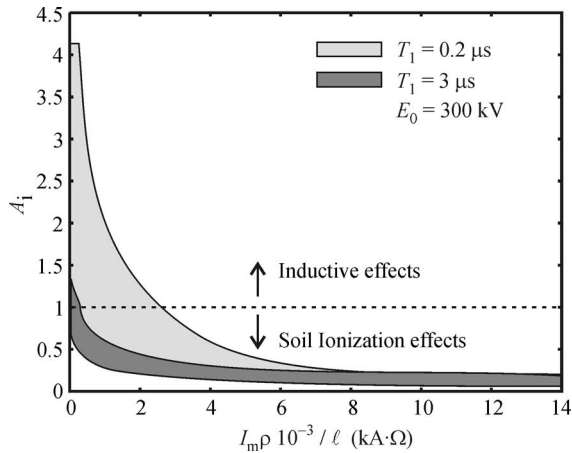


Fig. 22. Comparison between simulation results for impulse coefficient A_i for current pulses with front times $T_1 = 0.2 \mu\text{s}$ and $T_1 = 3 \mu\text{s}$.

effects. The presented simple computational procedure and (25) enable such an analysis (in their range of validity indicated in Table II). Fig. 22 shows the results of (25) for the same range of parameters as in Fig. 21, where results for two values of the lightning current pulse zero-to-peak time $T_1 = 3 \mu\text{s}$ is compared with $T_1 = 0.2 \mu\text{s}$. The shaded areas in Fig. 22 are the areas of the corresponding scattered results.

It is possible to distinguish combinations of parameters for which the inductive effects are dominant, i.e., when $A_i > 1$, and for which, the soil ionization effects are dominant, when $A_i < 1$. For the “slow” front current pulse with $T_1 = 3 \mu\text{s}$, there are practically no inductive effects, but for the fast front current pulse with $T_1 = 0.2 \mu\text{s}$, the induction effects start to nullify the soil ionization effects for the combination of parameters $I_m \rho \times 10^{-3}/l < 8 \text{ kA}\cdot\Omega$, and for small values of $I_m \rho \times 10^{-3}/l$, the inductive effects become dominant. In fact, three ranges of parameters $I_m \rho \times 10^{-3}/l$ can be distinguished: the range where soil ionization is dominant and independent of T_1 ($I_m \rho \times 10^{-3}/l > 8 \text{ kA}\cdot\Omega$), the range where the soil ionization and inductive effects nullify each other, and the range where the inductive effects are dominant.

IX. CONCLUSION

- 1) Two ranges can be distinguished in the frequency domain: the “low-frequency” range with dominantly resistive behavior and the “high-frequency” range with dominantly inductive or capacitive behavior. For any of the analyzed lengths of electrodes, there is a switch between inductive to capacitive behavior for more resistive earth. Inductive behavior is of special interest since it might impair performance in the early time of the lightning pulse. For such case, the key parameter is the switch frequency F_c between ranges of resistive and inductive behavior.
- 2) For the estimation of the performance in the first moments of the pulse, the frequency content of lightning current pulses is important (as a first approximation for the first stroke below 100 kHz, and for the subsequent stroke above 1 MHz). Inductive behavior impairs performance if such frequency content is above F_c .

- 3) The transient behavior during the lightning pulse can be divided into two periods: surge and stationary. The surge period lasts for a few or few tens of microseconds, and the stationary period up to the end of the pulse. The high-frequency behavior (inductive or capacitive) might have influence only in the surge period, while the stationary period is influenced by the low-frequency dominant resistive behavior.
- 4) Soil ionization has a small influence in the surge period in the case of inductive behavior, but has a dominant influence in the stationary period for currents with large peak values.
- 5) The circuit and the transmission-line models overestimate the computed potentials in comparison to the electromagnetic model in all considered cases. The differences are larger in case of inductive behavior, i.e., for longer electrodes and/or in more conductive earth. However, the differences last mostly during the surge period, and after that, results of the models mutually converge.
- 6) There exists a range of parameters where both soil ionization and inductive effects are important, and nullify each other.
- 7) The new simple formula might be used in combination with circuit and transmission-line models. The formula can be used to approximately determine the overestimation of the results in the surge period.

REFERENCES

- [1] V. A. Rakov and M. A. Uman, *Lightning, Physics and Effects*. Cambridge, U.K.: Cambridge Univ. Press, 2003.
- [2] *IEEE Guide for Safety in AC Substation Grounding*, IEEE Standard 80-2000, May 2000.
- [3] F. Rachidi, W. Janischewskyj, A. M. Hussein, C. A. Nucci, S. Guerrieri, B. Kordi, and J.-S. Chang, “Current and electromagnetic field associated with lightning-return strokes to tall towers,” *IEEE Trans. Electromagn. Comput.*, vol. 43, no. 3, pp. 356–367, Aug. 2001.
- [4] R. Rudenberg, *Electrical Shock Waves in Power Systems*. Cambridge, MA: Harvard Univ. Press, 1968.
- [5] L. Grcev, “Impulse efficiency of ground electrodes,” *IEEE Trans. Power Del.*, vol. 24, no. 1, pp. 441–451, Jan. 2009.
- [6] P. L. Bellaschi, R. E. Armington, and A. E. Snowden, “Impulse and 60-cycle characteristics of driven grounds—II,” *AIEE Trans.*, vol. 61, pp. 349–363, 1942.
- [7] K. Berger, “The behavior of earth connections under high intensity impulse currents,” in *Proc. CIGRE*, 1946, vol. 95, pp. 1–32.
- [8] A. C. Liew and M. Darveniza, “Dynamic model of impulse characteristics of concentrated earths,” *Proc. Inst. Electr. Eng.*, vol. 121, pp. 123–135, Feb. 1974.
- [9] J. Wang, A. C. Liew, and M. Darveniza, “Extension of dynamic model of impulse behavior of concentrated grounds at high currents,” *IEEE Trans. Power Del.*, vol. 20, no. 3, pp. 2160–2165, Jul. 2005.
- [10] R. Verma and D. Mukhedkar, “Impulse impedance of buried ground wire,” *IEEE Trans. Power App. Syst.*, vol. PAS-99, no. 5, pp. 2003–2007, Sep./Oct. 1980.
- [11] A. D. Papalexopoulos and A. P. Meliopoulos, “Frequency dependent characteristics of grounding systems,” *IEEE Trans. Power Del.*, vol. PWRD-2, no. 4, pp. 1073–1081, Oct. 1987.
- [12] L. Grcev and M. Heimbach, “Frequency dependent and transient characteristics of substation grounding system,” *IEEE Trans. Power Del.*, vol. 12, no. 1, pp. 172–178, Jan. 1997.
- [13] A. F. Otero, J. Cidras, and J. L. del Alamo, “Frequency-dependent grounding system calculation by means of a conventional nodal analysis technique,” *IEEE Trans. Power Del.*, vol. 14, no. 3, pp. 873–878, Jul. 1999.
- [14] Y. Liu, M. Zitnik, and R. Thottappillil, “An improved transmission-line model of grounding system,” *IEEE Trans. Electromagn. Comput.*, vol. 43, no. 3, pp. 348–355, Aug. 2001.

- [15] A. Geri, "Behaviour of grounding systems excited by high impulse currents: The model and its validation," *IEEE Trans. Power Del.*, vol. 14, no. 3, pp. 1008–1017, Jul. 1999.
- [16] J. Cidras, A. F. Otero, and C. Garrido, "Nodal frequency analysis of grounding systems considering the soil ionization effect," *IEEE Trans. Power Del.*, vol. 15, no. 1, pp. 103–107, Jan. 2000.
- [17] R. Zeng, X. Gong, J. He, B. Zhang, and Y. Gao, "Lightning impulse performances of grounding grids for substations considering soil ionization," *IEEE Trans. Power Del.*, vol. 23, no. 2, pp. 667–675, Apr. 2008.
- [18] V. Z. Annenkov, "Calculating the impulse impedance of long groundings in poor conducting soil," *Elektrichestvo*, no. 11, pp. 62–79, 1974.
- [19] C. Mazzetti and G. M. Veca, "Impulse behavior of grounded electrodes," *IEEE Trans. Power App. Syst.*, vol. PAS-102, no. 9, pp. 3148–3156, Sep. 1983.
- [20] R. Velazquez and D. Mukhedkar, "Analytical modeling of grounding electrodes," *IEEE Trans. Power App. Syst.*, vol. 103, no. 6, pp. 1314–1322, Jun. 1984.
- [21] P. Chowdhuri, *Electromagnetic Transients in Power Systems*. New York: Wiley, 1996.
- [22] L. Grcev and F. Dawalibi, "An electromagnetic model for transients in grounding systems," *IEEE Trans. Power Del.*, vol. 5, no. 4, pp. 1773–1781, Oct. 1990.
- [23] L. Grcev, "Computation of transient voltages near complex grounding systems caused by lightning currents," in *Proc. IEEE Int. Symp. Electromagn. Compat.*, 1992, pp. 393–399.
- [24] L. Grcev and F. Menter, "Transient electromagnetic fields near large earthing systems," *IEEE Trans. Magn.*, vol. 32, no. 3, pp. 1525–1528, May 1996.
- [25] L. Grcev, "Computer analysis of transient voltages in large grounding systems," *IEEE Trans. Power Del.*, vol. 11, no. 2, pp. 815–823, Apr. 1996.
- [26] *CIGRÉ Guide on Lightning Protection of MV and LV Networks: Part I Common Topics*, Int. Council Large Electr. Syst. (CIGRÉ), Paris, France, Tech. Brochure, 2006.
- [27] L. Grcev, "Impulse efficiency of simple grounding electrode arrangements," in *Proc. Int. Zurich Symp. Electromagn. Compat.*, Zurich, Switzerland, 2007, pp. 325–328.
- [28] L. Grcev and S. Grceva, "On HF circuit models of horizontal grounding electrodes," *IEEE Trans. Electromagn. Compat.*, vol. 51, no. 3, pp. 873–875, Aug. 2009.
- [29] H. B. Dwight, "Calculation of the resistances to ground," *Electr. Eng.*, vol. 55, pp. 1319–1328, Dec. 1936.
- [30] E. D. Sunde, *Earth Conduction Effects in Transmission Systems*, 2nd ed. New York: Dover, 1968.
- [31] S. Bourg, B. Sacepe, and T. Debu, "Deep earth electrodes in highly resistive ground: Frequency behaviour," in *Proc. 1995 IEEE Int. Symp. Electromagn. Compat.*, pp. 584–589.
- [32] C. T. Mata, M. I. Fernandez, V. A. Rakov, and M. A. Uman, "EMTP modeling of a triggered-lightning strike to the phase conductor of an overhead distribution line," *IEEE Trans. Power Del.*, vol. 15, no. 4, pp. 1175–1181, Oct. 2000.
- [33] F. Menter and L. Grcev, "EMTP-based model for grounding system analysis," *IEEE Trans. Power Del.*, vol. 9, no. 4, pp. 1838–1849, Oct. 1994.
- [34] A. Banos, *Dipole Radiation in the Presence of a Conducting Half-Space*. New York: Pergamon, 1966.
- [35] R. F. Harrington, *Field Computation by Moment Methods*. New York: Wiley-IEEE, 1993.
- [36] W. C. Gibson, *The Method of Moments in Electromagnetics*. Boca Raton, FL: CRC Press, 2007.
- [37] G. Burke and E. K. Miller, "Modeling antennas near to and penetrating a lossy interface," *IEEE Trans. Antennas Propag.*, vol. 32, no. 10, pp. 1040–1049, Oct. 1984.
- [38] A. V. Korsuntcev, "Application of the theory of similitude to the calculation of concentrated earth electrodes," *Elektrichestvo*, no. 5, pp. 31–35, May 1958.
- [39] E. E. Oettle, "A new general estimation curve for predicting the impulse impedance of concentrated earth electrodes," *IEEE Trans. Power Del.*, vol. 3, no. 4, pp. 2020–2029, Oct. 1988.
- [40] A. F. Imece, D. W. Durbak, H. Elahi, S. Kolluri, A. Lux, D. Mader, T. E. McDermott, A. Morched, A. M. Mousa, R. Natarajan, L. Rugeles, and E. Tarasiewicz, "Modeling guidelines for fast front transients," *IEEE Trans. Power Del.*, vol. 11, no. 1, pp. 493–506, Jan. 1996.
- [41] *CIGRÉ Guide to Procedures for Estimating the Lightning Performance of Transmission Lines*, Int. Council Large Electr. Syst. (CIGRÉ), Paris, France, Tech. Brochure, 1991.
- [42] L. Grcev, "Lightning surge characteristics of earthing electrodes," in *Proc. Int. Conf. Lightning Protection*, Uppsala, Sweden, 2008, pp. 1–16.
- [43] L. Grcev, "Time and frequency dependent lightning surge characteristics of grounding electrodes," *IEEE Trans. Power Del.*, to be published.
- [44] L. Grcev and M. Popov, "On high-frequency circuit equivalents of a vertical ground rod," *IEEE Trans. Power Del.*, vol. 20, no. 2, pp. 1598–1603, Apr. 2005.
- [45] C. Gary, "The impedance of horizontally buried conductors," in *Proc. Int. Symp. Lightning Mountains*, Chamonix-Mont-Blanc, France, 1994, pp. 148–151.
- [46] L. Grcev, "Improved earthing system design practices for reduction of transient voltages," presented at the CIGRE, Paris, France, 1998, Paper 36-302.
- [47] K. Berger, R. B. Anderson, and H. Kroninger, "Parameters of lightning flashes," *Electra*, vol. 80, no. 41, pp. 23–37, 1975.
- [48] B. R. Gupta and B. Thapar, "Impulse impedance of grounding systems," in *Proc. IEEE Power Eng. Soc. Summer Meeting*, 1978, pp. 1–6, Paper A 78 563-9.
- [49] J. He, R. Zeng, Y. Tu, J. Zou, S. Chen, and Z. Guan, "Laboratory investigation of impulse characteristics of transmission tower grounding devices," *IEEE Trans. Power Del.*, vol. 18, no. 3, pp. 994–1001, Jul. 2003.
- [50] H. Rochereau and B. Merheim, "Application of the transmission lines theory and EMTP program for modelisation of grounding systems in high frequency range," in *Collection de notes internes*. Paris, France: Electricité de France (EDF) Direction des Etudes et Recherches (DER), 1993, p. 21, Note 93NR00059.
- [51] E. Y. Ryabkova and V. M. Mishkin, "Impulse characteristics of high voltage transmission line tower groundings in homogeneous soil," *Elektrichestvo*, no. 8, pp. 67–70, 1976.
- [52] Saint-Privat-d' Allier Research Group, "Eight Years of lightning experiments at Saint-Privat-d' Allier," *Rev. Gen. de l'Electr.*, vol. 91, no. 9, pp. 561–582, Sep. 1982.
- [53] D. Roubertou, J. Fontaine, J. P. Plumey, and A. Zeddami, "Harmonic input impedance of earth connections," in *Proc. 1984 IEEE Int. Symp. Electromagn. Compat.*, pp. 717–720.
- [54] A. J. Eriksson and K. H. Weck, "Simplified procedures for determining representative substation impinging lightning over voltages," in *Proc. CIGRE Session*, Paris, France, 1988, pp. 1–8, Paper SC33-16.
- [55] A. M. Mousa, "The soil ionization gradient associated with discharge of high currents into concentrated electrodes," *IEEE Trans. Power Del.*, vol. 9, no. 3, pp. 1669–1677, Jul. 1994.
- [56] *Handbook for Improving Overhead Transmission Line Lightning Performance*. Electr. Power Res. Inst. (EPRI), Palo Alto, CA, Rep. 1002019, 2004.



Leonid Grcev (M'84–SM'98) was born in Skopje, Macedonia, in 1951. He received the Dipl. Ing. in electrical engineering from Ss. Cyril and Methodius University, Skopje, in 1978 and the M.Sc. and Ph.D. degrees in electrical engineering from the University of Zagreb, Zagreb, Croatia, in 1982 and 1986, respectively.

From 1978 to 1988, he was with the Telecommunications Department, Electric Power Company of Macedonia, Skopje. He is currently a Full Professor with the Faculty of Electrical Engineering, Ss. Cyril and Methodius University, where since 1988, he has also been an Assistant Professor, an Associate Professor, and the Vice Dean. He has been a Visiting Professor at the Technical University of Aachen, Aachen, Germany, the Eindhoven University of Technology, Eindhoven, The Netherlands, and the Swiss Federal Institute of Technology, Lausanne, Switzerland. He was engaged in several international projects related to electromagnetic compatibility (EMC). He has authored or coauthored many scientific papers published in reviewed journals and presented at international conferences. His current research interests include high-frequency and transient grounding, lightning, EMC, high-power electromagnetics, bioelectromagnetics, and electromagnetic field health effects.

Prof. Grcev is a member of the International Council on Large Electric Systems (CIGRE) Working Groups related to EMC and lightning protection.